PAPER • OPEN ACCESS

Quantum illumination assistant with error-correcting codes

To cite this article: Wen-Zhao Zhang *et al* 2020 *New J. Phys.* **22** 013011

New Journal of Physics
The open access journal at the forefront of physics

Deutsche Physikalische Gesellschaft DPG
IOP Institute of Physics

Published in partnership with: Deutsche Physikalische Gesellschaft and the Institute of Physics

OPEN ACCESS

RECEIVED
21 August 2019

REVISED
29 November 2019

ACCEPTED FOR PUBLICATION
10 December 2019

PUBLISHED
14 January 2020

PAPER

Quantum illumination assistant with error-correcting codes

Wen-Zhao Zhang[1], **Yu-Han Ma**[1], **Jing-Fu Chen**[1] and **Chang-Pu Sun**[1,2]

[1] Beijing Computational Science Research Center (CSRC), Beijing 100193, People's Republic of China
[2] Graduate School of Chinese Academy of Engineering Physics, Beijing 100084, People's Republic of China

E-mail: cpsun@csrc.ac.cn

Keywords: quantum illumination, error-correcting codes, quantum optics

Abstract

We scheme how to enhance the detection ability of quantum target recognition without using entanglement resources. Based on the commonly used error-correcting codes and corresponding decoding method, our scheme gives lower error probability and higher signal-to-noise ratio (SNR) in comparison with the conventional entanglement protocols. In addition, we further investigate the interplay between the SNR and the detection efficiency in quantum target recognition. Results show that, they behave a completely reverse trend when increasing the auxiliary dimension. This is an important limiting factor when optimizing the detection process. Under the existing experimental conditions, our protocol has stronger ability to resist environmental noise when keeping a certain SNR and detection efficiency. Our scheme provides a potential platform for further research and implementation of quantum target recognition.

1. Introduction

Target recognition is the core element in radar system. The properties of quantum states have disclosed the possibility of realizing this task beyond classical limits [1–3]. One of the major applications to enhance the ability of target recognition is quantum illumination [4–9], which is the most known protocol for bosonic quantum sensing [10]. Quantum illumination provides us with a potential platform to detect the low-reflectivity object embedded in a bright environment, and it is more efficiently than the way by using classical resources [5, 11, 12]. Since the pioneering work proposed by Lloyd [4] and its Gaussian version [6, 9], many experimental and theoretical schemes have been proposed [13, 14], such as quantum illumination in composite optomechanical system [5, 15], discrete variable quantum illumination with ancillary degrees of freedom [16], quantum illumination unveils cloaking [14], and quantum illumination based on asymmetric hypothesis testing [17, 18]. In these researches, quantum entanglement and quantum correlation are the necessary resources to reduce the error probability of target recognition. This means the lower error probability requires the higher dimension of entangled state [4], which pose a great challenge to the experimental implementation. Various schemes have been proposed to improve the feasibility of experiment, including quantum illumination with Gaussian state entanglement [6], quantum illumination combined with quantum estimation methods [11], and so on. Most recently, a fundamental lower bound of error probability of quantum illumination for both discrete variable [19] and continuous variable [20] systems have been reported. Up to now, most of the quantum illumination schemeswere still based on the nonclassical correlations between signal and idler beams [13–16]. In that case, the enhancement of detection ability is at the expense of the quantum correlation between signal photons and auxiliary photons. Since the high dimensional quantum correlation is hard to realize in experiment, the schemes based on quantum illumination will unavoidably limit the improvement of the signal-to-noise ratio (SNR) [14–16, 21].

In order to reduce environmental noise, besides quantum correlation, the signal coding is also an effective way, which has been widely applied in quantum communication [22]. For example, using the error-correcting codes (ECC) to enhance the discernibility between signals and noise [23]. For quantum target recognition, to obtain higher signal discriminability, one can introduce an auxiliary system used for coding. As we know, it is

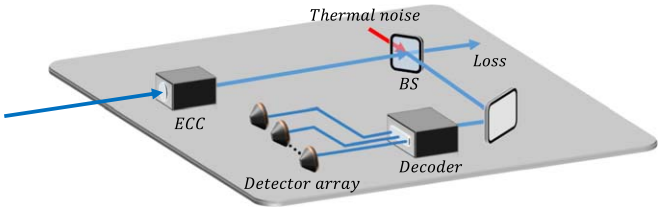

Figure 1. Diagrammatic sketch of quantum target recognition based on ECC protocol. The input signal is encoded by the 'ECC' and prepared as the emitted state to illuminate the object modeled as a beam splitter (BS). The reflected signal is injected into the decoder and then be detected by the detection array.

much easier to encode the initial state than to prepare the high-dimensional entangled state [24] in experiment. In ECC, signal state and auxiliary states can be written in direct product form, which does not contain quantum correlation.

In view of this fact, we investigate the SNR of the quantum target recognition based on the ECC on the emitted state. The corresponding detection scheme is designed to reduce the error probability and enhance the SNR in quantum target recognition. In addition, we also investigate the relationship between the SNR and the detection efficiency p, which shows a completely reverse trend.

The remainder of this paper is as follows. In section 2, we describe the detection scheme of the quantum target recognition based on the ECC and discuss the detection error probability bound. In section 3, we exhibit the SNR enhancement ability of our scheme by comparing with the original protocol [4]. In section 4, we investigate the relationship between the SNR and the detection efficiency p in quantum target recognition. Finally, we conclude in section 5.

2. Quantum target recognition based on ECC

Quantum illumination has became a most common way to study quantum target recognition. Associating quantum correlation sources with quantum measurement methods, quantum illumination exhibits excellent capability to enhance SNR in quantum target recognition. Another effective approach to quantum target recognition is built on the quantum key distribution (QKD). The detection object is modeled as a kind of losing channel [25, 26]. This model can be used to discuss the extended properties of quantum target recognition, such as security [25]. In this section, a simplest ECC is used in QKD instead of entanglement state in the initialization of quantum illumination is discussed. The setup of our scheme is shown in figure 1. The input signal is encoded into the state $|\psi\rangle_E = |1\rangle_1|1\rangle_2...|1\rangle_d = \Pi_k a^\dagger(k)|\text{vac}\rangle$, where d is the dimension of coding. This state is naturally normalized. $|\psi\rangle_E$ is prepared as the emitted state to illuminate the object. The received signal is injected into the decoder and then be detected by the detection array. Only when all detectors have a single photon response, the object can be regarded is there, otherwise it will be regarded as noise (other error-correction coding methods are discussed in appendix C).

In comparison with entanglement protocol in [4], we let signal photons of each mode to possess the same level of thermal noise. The corresponding environment can be described as

$$\wp_{\text{th}} = \prod_{k=1}^{d} \rho_{\text{th}}(k), \tag{1}$$

where $\rho_{\text{th}}(k) = \sum_n n_{\text{th}}^n/(n_{\text{th}}+1)^{n+1}|n_k\rangle\langle n_k|$ denotes the thermal environmental density operator of the kth model, n_{th} is the average excitation number of thermal noise. The signal state is sent at the object to be detected. The signal is reflected back mixed with the background noise. The dynamics corresponding to this situation can be modeled as beam splitter (BS) with reflectivity η [6]. To better explore the parametric dependence of our scheme, we do not adapt the commonly used approximation methods to simplify the calculation [4]. As follows, we set the nonthermal noise can be tolerated and then study the corresponding quantum illumination based on the accurate calculation of quantum BS model (details see appendix A). In our protocol, the constructed state for signal photon and ancilla photons are send to toward the object which is modeled as a BS. The two different dynamics corresponding to object (C_0) or no object (C_1) now take a different form because the interaction of the object must be included. If the signal photon is lost, the reflected photon goes to the completely mixed state. Thus, in our model, the target recognition is equivalent to distinguishing two situations C_0 and C_1. In case C_0, the signal can not return to the decoder, i.e. the reflectivity rate $\eta = 0$ in figure 1. Under this condition, the received signal is totally from the thermal radiation. The received state can be expressed as,

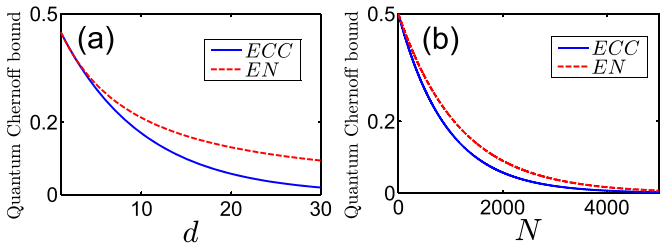

Figure 2. Quantum Chernoff bound as a function of auxiliary dimension d in (a), and number of copies of signals N in (b). The parameters are $\eta = 0.01$, $n_{th} = 0.1$, $N = 1000$ and $d = 10$.

$$\rho_{r0} = |\mathrm{vac}\rangle_s \langle \mathrm{vac}| \otimes \wp_{\mathrm{th}}, \tag{2}$$

subscript s denotes the subspace of the signal photons. In case C_1, without considering the transmission dissipation, the initial state before interact with object can be expressed as $\rho_i = \prod_{k=1}^{d} |1\rangle_k \langle 1| \otimes \wp_{\mathrm{th}}$. After scatting by the object, the thermalized signal photons return to the decoder. The corresponding mixed state can be expressed as,

$$\rho_{r1} = \prod_{k=1}^{d} \rho_r(k), \tag{3}$$

where

$$\begin{aligned}\rho_r(k) = &\sum_{j}^{n_k} \sum_{n_k} \frac{n_{\mathrm{th}}^{n_k}}{(n_{\mathrm{th}}+1)^{n_k+1} n_k!} \{C_{n_k}^{j} \eta^{n_k-j}(1-\eta)^j \times j!(n-j+1)![C_{n_k}^{j}(1-\eta) - C_{n_k}^{j-1}\eta]|j\rangle\langle j| \\ &+ C_{n_k}^{j} \eta^{n_k-j+2}(1-\eta)^j (j+1)!(n-j)! \times [C_{n_k}^{j}\eta - C_{n_k}^{j+1}(1-\eta)]|j+1\rangle\langle j+1|\} \\ = &\sum_{n_k} p'(n_k)|n_k\rangle\langle n_k|. \end{aligned} \tag{4}$$

The considered detection probability of the received state in our scheme can be expressed as

$$p'(1) = \frac{n_{\mathrm{th}}(1+n_{\mathrm{th}})(1-\eta)^2 + \eta}{[1+(1-\eta)n_{\mathrm{th}}]^3}. \tag{5}$$

To distinguishing two cases C_0 and C_1, we should discrimination between the quantum state ρ_{r0} and ρ_{r1}. The quantum Chernoff bound [27] is the natural symmetric distance measure between quantum states, and the general definition is given by $P_{QC} = 1/2 \min_{s\in[0,1]} \mathrm{tr}\rho_{r0}^{s}\rho_{r1}^{1-s}$ [28]. The quantum Chernoff bound gives a tighter bound than that given by the quantum fidelity [29]. The relationship between them follows from the following set of inequalities:

$$P_{QC} = \frac{\min\limits_{s\in[0,1]} \mathrm{tr}\rho_{r0}^{s}\rho_{r1}^{1-s}}{2} \leqslant \frac{\mathrm{tr}\rho_{r0}^{1/2}\rho_{r1}^{1/2}}{2} \leqslant \frac{\mathrm{tr}|\sqrt{\rho_{r0}}\sqrt{\rho_{r1}}|}{2} = \frac{\sqrt{F(\rho_{r0},\rho_{r1})}}{2}, \tag{6}$$

where $F(\rho_{r0}, \rho_{r1})$ is the widely used quantum fidelity [30], the matrix $|\rho|$ is defined to be $|\rho| = \sqrt{\rho^{\dagger}\rho}$. In our scheme, the quantum Chernoff upper bound (QCB) [27, 28] limits the asymptotic error probability when N copies of signals are sent at the object [28, 29], it is shown that,

$$P_{\mathrm{err}} = \frac{1}{2}\left(1 - \frac{1}{2}\mathrm{tr}|\rho_{r1}^{\otimes N} - \rho_{r0}^{\otimes N}|\right) \leqslant \frac{1}{2}\exp\left\{N\left[\min_{s\in[0,1]} \log\mathrm{tr}\rho_{r0}^{s}\rho_{r1}^{1-s}\right]\right\} = \frac{1}{2}Q_C^N. \tag{7}$$

Under the condition $n_{\mathrm{th}} \ll 1, \eta \ll 1$, the coefficient Q_C in our scheme can be obtained,

$$Q_C \approx \min_{s\in[0,1]} (1-\eta)^{sd} \times \left\{1 + n_{\mathrm{th}}\left[-1 + \left(1 + \frac{\eta}{n_{\mathrm{th}} - \eta n_{\mathrm{th}}}\right)^{s}\right]\right\}^{d}. \tag{8}$$

Figure 2 shows the numerically simulate of the quantum Chernoff bound of our scheme and the original quantum illumination scheme [4]. As shown in figure 2(a), the number of copies of signal is $N = 1000$. The boundaries of the two schemes will decrease significantly with the increase of auxiliary dimension d. When d is large enough the boundary of our scheme is much lower than that of original one. Thus, our scheme has more advantages by reducing the error probability through the auxiliary dimension by comparing with the original protocol [4]. As shown in figure 2(b), as the number of copies increases, the bound of both schemes gradually decreases. When N is large enough, the bound tends to zero. Under this condition, the object can be deterministic recognized.

One should notice that, the QCB is a theoretical state distance, which is similar to the definition of quantum fidelity only depends on the form of two density operators. The two density operators can be distinguished only under the condition there are enough copies, and all the bases of density operators can be measured perfectly. In addition, for quantum illumination, the received states are an unknown state, and it cannot be copied perfectly. Therefore, the discussion of QCB in the figure 2 is to analyze the capability based on different emitted state without considering the detection protocols. In the following discussion, we only consider the SNR of single detection without copies in quantum illumination schemes.

3. The enhancement of SNR

Quantum Chernoff bound is one of the evaluation methods for quantum illumination [4, 6, 9]. But it is not a universal evaluation standard in conventional target recognition system. The commonly used SNR in detection [31–33] need to be considered to evaluate the advantages of quantum target recognition scheme. According to the analysis in section 2, there are two possible cases of the output signal shows object is there, i.e. C_0 and C_1. For the case C_0, it is a misleading feedback information, the fact that the object is not there. Thus, the received photons under this situation is noise. Performing projection measurements on a single photon detector array, the corresponding detection probability with the response of the object is there can be obtained

$$p(0|Y) = \left[\frac{n_{\rm th}}{(1+n_{\rm th})^2}\right]^d, \tag{9}$$

$$p(1|Y) = p'^d(1). \tag{10}$$

According to the general definition of SNR,

$$\mathrm{SNR}_C = \left\{\frac{(1+n_{\rm th})^2[n_{\rm th}(1+n_{\rm th})(1-\eta)^2+\eta]}{n_{\rm th}[1+(1-\eta)n_{\rm th}]^3}\right\}^d. \tag{11}$$

In equation (11), one can obtain that $\mathrm{SNR}_C(d=1) \geqslant 1$. When $n_{\rm th}=0$, denotes that there is no noise in detection. Under this condition $\mathrm{SNR}_C = \infty$, the object can be detected accurately. When $\eta = 0$, denotes that there is no signal in detection. Under this condition $\mathrm{SNR}_C = 1$, it is impossible for us to judge whether the object exists or not.

According to equation (11), SNR_C increases exponentially with dimension d. This should be compared to the result of the traditional entanglement (EN) protocol [4], where

$$\mathrm{SNR}_E = \frac{1+(n_{\rm th})^{d+1}[n_{\rm th}(1+n_{\rm th})(1-\eta)^2+\eta d]}{n_{\rm th}[1+n_{\rm th}(1-\eta)]^{d+2}}. \tag{12}$$

Equation (12) is an the exact solution of the entanglement protocol (details see appendix A). The conclusion $\mathrm{SNR}_E \sim \eta d/n_{\rm th}$ in [4] can be obtained under the condition $n_{\rm th} \ll 1$ and $\eta \ll 1$. It is obvious that, SNR increases linearly with dimension d. Comparing equation (11) with (12), ECC scheme has more advantages than EN scheme in improving SNR. In addition, the SNR_E can not be enhanced by a large number of copies of the initial state under the given detection scheme in [4], i.e. $\mathrm{SNR}_E^{(N)} \leqslant \mathrm{SNR}_E$ (details see appendix A).

Figure 3 shows the comparison of the SNR enhancement ability of our scheme with the traditional EN scheme. As shown in figure 3(a), the SNR obviously increases with d for both schemes. The curve of ECC is much higher than that of EN. Under the given parameters $n_{\rm th} = 0.1$ and $\eta = 0.01$, SNR approximately reach 36 in ECC protocol, and about 6 in EN protocol. As shown in figure 3(b), the SNR increases with the increase of reflectivity rate η. The enhancement of SNR of ECC scheme is also much better than that of EN scheme. Figures 3(c) and (d) shows the impact of thermal environment temperature on quantum target recognition. As shown in figure 3(c), under the condition the thermal noise is much lesser than 1, the SNR decreased sharply with the increase of $n_{\rm th}$. For ECC protocol, the SNR decreases much slower than EN protocol. As shown in figure 3(d), with the continue increase of $n_{\rm th}$, SNR decreases first and then increases. Finally, SNR of both schemes tend to a certain value. This is because the probability of detecting a single photon has a maximum value (about 0.25) when $n_{\rm th} \approx 1$ under the Case C_0. Thus there is a minimum value of SNR. Under the given parameters, when $n_{\rm th}$ is much greater than 1, we can obtain that the SNR of ECC and EN protocols are approximately equal to $1/(1-\eta)^d$, i.e. SNR ≈ 1.1 under the given parameters. When $n_{\rm th}$ is large enough, EN protocol has a slight advantage in anti-noise ability, but the ability of SNR enhancement for both protocols is very small.

Under high temperature conditions, ECC scheme needs a higher dimension than EN scheme to achieve the same SNR under the large background noise. The comparison is shown in figures 4(a) and (b). When $n_{\rm th} = 10$, to achieve SNR $= 2$, $d = 94$ is needed in ECC scheme and $d = 76$ is needed in EN scheme. In addition, the larger the $n_{\rm th}$ is, the higher the SNR is. Because, under high temperature condition, the signal intensity is

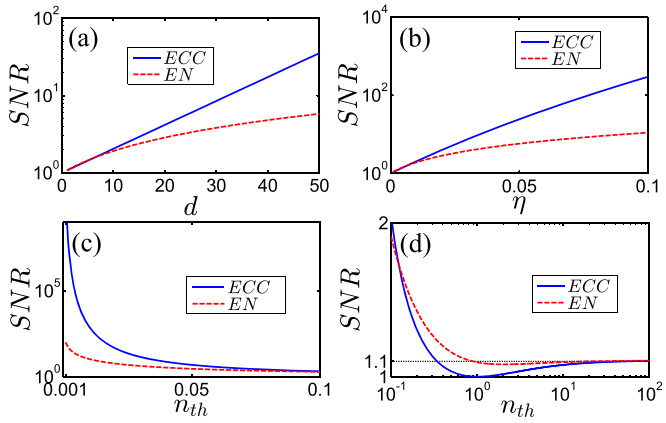

Figure 3. SNR as a function of dimension d, reflection rate η and average thermal number $n_{\rm th}$ with different schemes. The parameters are $n_{\rm th} = 0.1, \eta = 0.01, d = 10$.

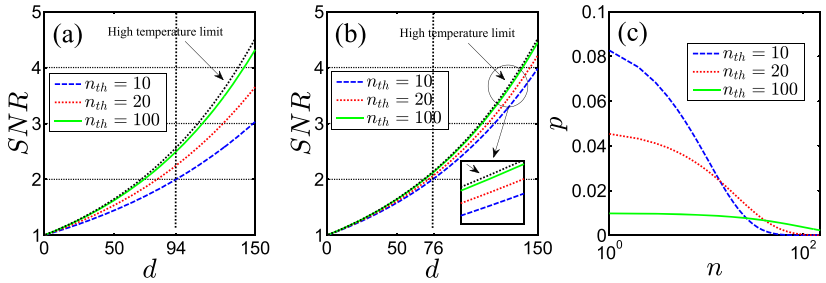

Figure 4. (a) and (b) denotes the SNR of ECC and EN as a function of dimension d, respectively. (c) Denotes the probability distribution of photons in the thermal state. The reflectivity rate $\eta = 0.01$.

approximately equal to constant, and the noise intensity depends on the component of $|1\rangle$ in thermal state. According to figure 4(c), the larger the thermal noise is, the smaller the superposition coefficient of $|1\rangle$ is. Therefore, SNR will reach the high temperature limit with the increase of $n_{\rm th}$.

It is worth noting that the comparison of ECC scheme and EN scheme are both under the same dimension d. In the experiment realization, the high dimension of ECC is much easier to realize than high dimension entanglement state. Therefore, our ECC scheme has greater potential advantages in practical application.

In our scheme, target recognition is equivalent to the process of identifying entangled states and thermal states after entanglement purification. This can be proved by using the conclusions in [34, 35], which relating the QKD to entanglement purification and quantum ECC. In addition, the non-Fock state will add a probability factor far less than 1 in the detection. We compared the SNR of ECC based on Fock state and coherent state (classical ECC) in figure 5. As shown in figure 5(a), ECC scheme based on Fock state is obviously better than that based on coherent state. Because in the single photon detection, the superposition coefficient of Fock state is 1 and the superposition coefficient of coherent state is less than 1. For coherent states , the larger α is, the smaller the superposition coefficient in front of is. Thus, the corresponding SNR is lower. In addition, the SNR of all schemes will approach 1 when the thermal noise is large enough, which is consistent with the previous conclusion. As shown in figure 5(b), with the increase of dimension, SNR based on Fock state increases obviously, but SNR based on coherent state decreases obviously due to the existence of superposition coefficient less than 1. Therefore, in ECC scheme, the closer the emission state is to the Fock state, the higher the SNR is.

In our model, through the interaction of BS, signal photons are mixed with the thermal photons. The useful information is distributed in different bases of photon number state with certain probability. Thus, to make use of information in the reflective signal photons and to facilitate our detection, the detected non-zero signals is considered as useful signal responses. Namely, when the detector array responds to non-zero signals, we regard the object is there. Under this condition, the corresponding detection probability of response the object is there can be obtained

$$p(0|Y) = \left(1 - \frac{1}{1 + n_{\rm th}}\right)^d, \tag{13}$$

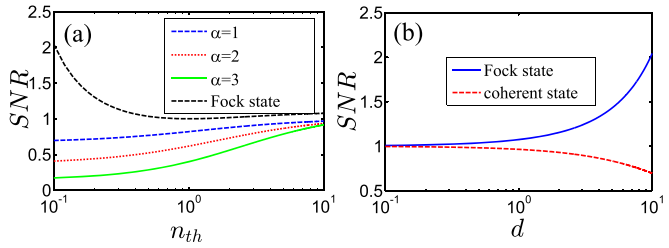

Figure 5. (a) SNR as a function of thermal number $n_{\rm th}$ with different ECC schemes. Black dashed line denotes ECC scheme based on Fock state. Other lines denote ECC scheme based on coherent state with different α. (b) SNR as a function of dimension d with different ECC schemes. The parameters are $n_{\rm th} = 0.1, \eta = 0.01, d = 10$.

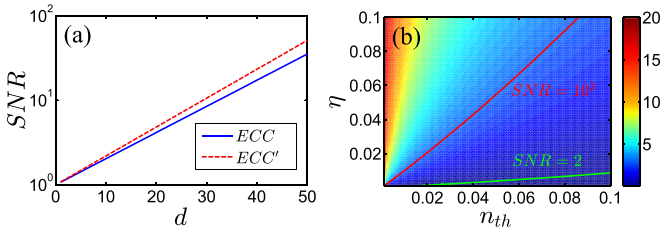

Figure 6. (a) SNR as a function of dimension d with ECC scheme and improved ECC scheme. $\eta = 0.01$ and $n_{\rm th} = 0.1$. (b) SNR (in the logarithmic scale) as a function of reflection rate η and average thermal number $n_{\rm th}$. The coding dimension $d = 10$.

$$p(1|Y) = \left[1 - \frac{(1 + n_{\rm th})(1 - \eta)}{(1 + n_{\rm th} - \eta n_{\rm th})^2}\right]^d. \tag{14}$$

The corresponding SNR is

$$\mathrm{SNR}'_C = \left\{\frac{(1 + n_{\rm th})[n_{\rm th}^2(1 - \eta)^2 + n_{\rm th}(1 - \eta) + \eta]}{n_{\rm th}[1 + n_{\rm th}(1 - \eta)]^2}\right\}^d. \tag{15}$$

Figure 6(a) shows the comparison of SNR in ECC scheme with the improved detection method and the original method. Due to the use of high excited photons' information, the SNR of improved scheme have been enhanced compared with the original measurement method.

Figure 6(b) shows the enhancement of SNR for different thermal noise and reflectivity rate with improved ECC protocol. As shown in the area near the green line in the figure, i.e. high noise and low reflectivity condition, the enhancement of SNR is rather weak. As shown in the area near the red line in the figure, i.e. low noise and high reflectivity, the enhancement of SNR is very strong. Thus, entanglement is not a necessary resource to enhance SNR in quantum target recognition. Anti-noise protocols like ECC in quantum information also can achieve the same effect.

4. Constraint relation of SNR and detection efficiency

To evaluate the performance of the object detection, not only the enhancement of SNR, but also the detection efficiency p [33] should be considered. Detection efficiency denotes the detection response rate and energy consumption of the recognition system, i.e. $p(1|Y)$. According to the analysis in section V, the enhancement of SNR requires the sacrifice of the assisted photons. Similar relationship also can be found in heat engines [36]. To reveal the relationship between SNR and the detection efficiency, without losing its generality, we define the normalized SNR as,

$$\widetilde{\mathrm{SNR}} = 1 - e^{1-\mathrm{SNR}}, \ \widetilde{\mathrm{SNR}} \in [0, 1]. \tag{16}$$

Figure 7(a) shows the p and $\widetilde{\mathrm{SNR}}$ as the function of dimension d. $\widetilde{\mathrm{SNR}}$ increases with the increases of dimension, while p decreases. Compared with EN protocol (red-line) and ECC protocol (blue-line), the SNR of ECC protocol increases faster than the EN protocol, while the detection efficiency of ECC protocol decreases faster than that of EN protocol with the increase of dimension. For ECC protocol, SNR improves and p decreases with

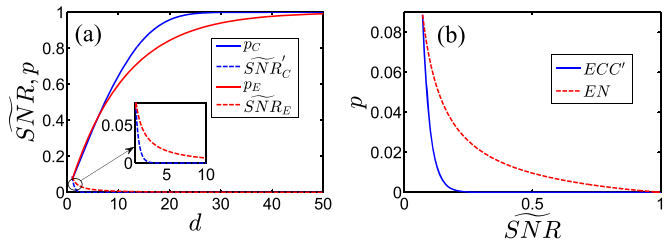

Figure 7. (a) $\widetilde{\mathrm{SNR}}$ and p as a function of dimension d with different protocols. (b) Detection efficiency p as a function of $\widetilde{\mathrm{SNR}}$ with different protocols. The reflectivity of detection object is $\eta = 0.01$, the thermal number is $n_{\mathrm{th}} = 0.1$.

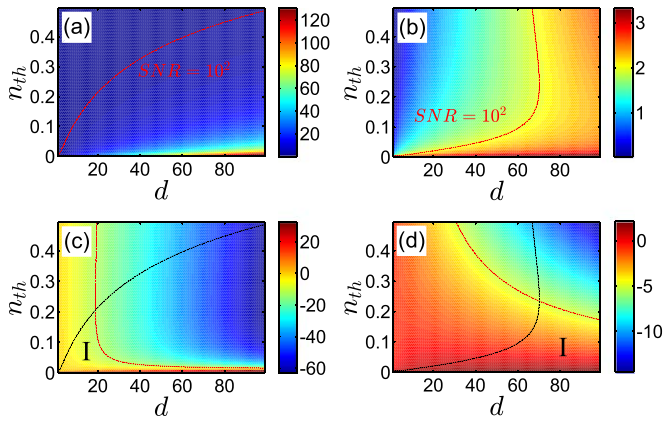

Figure 8. (a) and (b) SNR (in the logarithmic scale) as a function of n_{th} and d with ECC protocol and EN protocol, respectively. The red-line denotes $\mathrm{SNR} = 10^2$. (c) and (d) $\mathrm{SNR} \times p$ (in the logarithmic scale) as a function of n_{th} and d with ECC protocol and EN protocol, respectively. (c) The red-line denotes $G_C = 10^{-12}$. (d) The red-line denotes $G_E = 10^{-5}$. The reflection rate $\eta = 0.1$.

the increase of the dimension. The improvement of $\widetilde{\mathrm{SNR}}$ for both schemes are accompanied by the decrement of p, which is consistent with the previous analysis.

As shown in figure 7(b), the detection efficiency p of ECC scheme is much lower than that of EN protocol under the same SNR. On the other hand, the SNR of EN protocol is much higher than that of ECC protocol under the same detection efficiency. When SNR approaches to 1, the detection efficiency of the two protocols are approaches to 0. Thus, the comprehensive performance of EN protocol is better than that of ECC protocol when the experimental implementation is ignored.

According to the analysis of figure 7, SNR and p shows obvious opposite dependence relationship between each other. It is similar with Heisenberg's relation. Thus the product of SNR and p can be used to express this relationship, i.e. $G = \mathrm{SNR} \times p$. Returning to the original definition of SNR, G with different protocols can be expressed as,

$$G_C = \mathrm{SNR}'_C \times p'_C = \left\{ \frac{(1 + n_{\mathrm{th}})[n_{\mathrm{th}}(1-\eta)(1 + n_{\mathrm{th}} - n_{\mathrm{th}}\eta) + \eta]^2}{n_{\mathrm{th}}[1 + n_{\mathrm{th}}(1-\eta)]^4} \right\}^d, \tag{17}$$

$$G_E = \mathrm{SNR}_E \times p_E = \frac{(1 + n_{\mathrm{th}})^{d+1}[n_{\mathrm{th}}(1 + n_{\mathrm{th}})(1-\eta)^2 + d\eta]^2}{d n_{\mathrm{th}}[1 + n_{\mathrm{th}}(1-\eta)]^{2(d+2)}}. \tag{18}$$

It is shown that, when the reflectivity η is close to 1, both SNR and p will be achieved to an optimal value. When the reflectivity is rather low, the situation becomes very complicated. Under the condition $\eta \ll 1$

$$G'_C \approx \left[\frac{n_{\mathrm{th}}}{(1 + n_{\mathrm{th}})^2} \right]^d, \tag{19}$$

$$G_E \approx \frac{n_{\mathrm{th}}}{d(1 + n_{\mathrm{th}})^{d+1}}. \tag{20}$$

The upper bound of G of both schemes decrease with dimensions obviously. The appropriate selection of SNR and p should be made according to actual needs. The influence of SNR with different dimension d and thermal number n_{th} for ECC and EN schemes are displayed in figures 8(a) and (b), respectively.

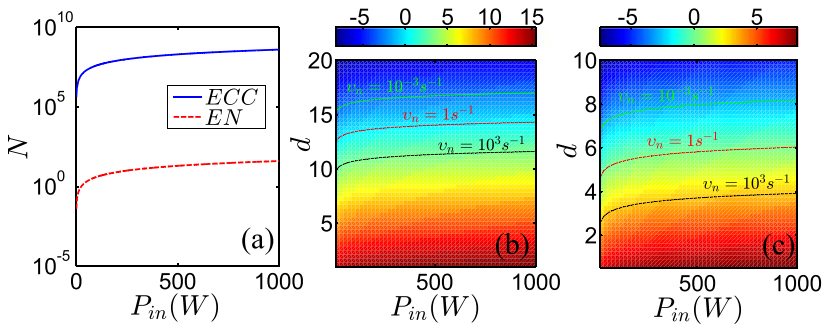

Figure 9. (a) Copy limit N of the initial state as a function of input power with ECC and EN schemes. The dimension $d = 10$. (b) and (c) Detection rate (in the logarithmic scale) as a function of dimension d and input power P_{in} with ECC protocol and EN protocol, respectively. The reflection rate $\eta = 0.01$, thermal number $n_{\text{th}} = 0.1$.

Compared with figures 8(a) and (b), the ECC scheme has obvious advantages over the EN protocol. The SNR of ECC scheme can achieve higher value than that of EN scheme. The red-dotted line in figures 8(a) and (b) indicates SNR $= 100$. It is shown that, ECC scheme has better anti-noise performance in low-dimensional case and EN protocol has more advantage in the high-dimensional case. Under the given object (reflectivity), for different levels of noise, if we require SNR > 100, we need to select the dimension corresponding to the right side of the red-dotted line in figures 8(a) and (b). In experiments, the realization of single photons is much easier than that of entangled photons. According to [37], using 710 nm driven laser, the efficiency of single photons generation in a nonlinear medium is 10^{-5}. For entangled photons, the reported generation efficiency with type-II phase-matched spontaneous parametric down-conversion is 10^{-12} [38] under 775 nm driven laser. For high-dimensional entanglement state, this efficiency is much lower. The efficiency we discussed here refers to the ratio of the total energy of the output photons we need to the total energy of the input field. The influence of G with different n_{th} and p for ECC and EN schemes are displayed in figures 8(c) and (d), respectively. For fair comparison, the red-dotted line in figure 8(c) denotes $G_C = 10^{-12}$, and the red-dotted line in figure 8(d) denotes $G_E = 10^{-5}$. Combined with the parameter range of SNR > 100 in figures 8(a) and (b) (the black-dotted line). The region I indicates that the signal photons with SNR higher than 100 and received rate more than $4000/J$ under given parameters in [37, 38] (details see appendix D). Compared with figures 8(c) and (d), under the low dimension region the ECC protocol has better anti-noise capability, and under the high dimension region the EN protocol is much better.

In figure 9(a), we explore the copy limit of the initial state of EN protocol and ECC protocol in nanosecond detector, respectively. The discussion is under experimental condition reported in [37, 38]. It is shown that, the copy limit of two protocols increases with the increase of input power P_{in}. ECC protocol has obvious advantages over EN protocol. In addition, we investigate the relationship between the detection rate υ_n of the two protocols in figures 9(b) and (c), respectively. It is shown that, the detection rate decreases with the increase of dimension, which is consistent with the conclusion of detection efficiency in the previous discussion. Combined with figures 9(b) and (c), we find that ECC protocol has a higher detection rate than EN protocol under the same input power and dimension. From the experimental point of view, high dimensional entanglement is difficult to be realized and maintained. Thus, our protocol has more advantages under the current experimental conditions.

5. Conclusion

As summary, a scheme based on ECC was proposed to reduce the quantum Chernoff bound and enhance the SNR in quantum target recognition. Compared with the original EN protocol,the ECC scheme shows an excellent detection ability in target recognition. Since it can achieve higher anti-noise effect when detecting low-reflection object. The detection SNR exponentially increases with the auxiliary code dimension in our scheme. Under the consideration of the experimental realization, the required quantum resources with single photon state in our scheme is much feasible to be realized than that with entanglement sate in commonly used quantum illumination protocol. In addition, the relationship between SNR and detection efficiency p in quantum target recognition is investigated. The result shows a completely opposite trend as the increase of auxiliary dimension. High SNR offer high detection accuracy and high p can offer high detection efficiency. The values of SNR and p need to be balanced. Using the parameters in [37, 38] as illustration, we show the selection of SNR and p in detail. Under the given condition ($\eta = 0.1$) and requirements (SNR > 100,

receiving rate $> 4000/J$), our protocol has more advantages in the low-dimensional case ($d < 40$), while EN protocol is better in the high-dimensional case ($d > 40$). In fact, it is difficult to prepare and preserve high-dimensional quantum resources, especially high-dimensional entanglement. Therefore, with the current experimental conditions, our scheme is more executable and it provides a new platform to improve the performance of quantum target recognition.

Acknowledgments

Project supported by the National Natural Science Foundation of China (Grant Nos. 11704026, 11704205, 11847128, U1530401), the China Postdoctoral Science Foundation funded project (Grant No. 2018T110039) and the Natural Science Foundation of Ningbo (Grant No. 2018A610199).

Appendix A. Accurate calculation of quantum BS model

For quantum BS, by setting the input ports are 0 and 1, and the output ports are 2 and 3, one can obtain the corresponding operators satisfy the following relations,

$$a_1 \xrightarrow{\text{BS}} ira_2 + ta_3, \tag{A.1}$$

$$a_0 \xrightarrow{\text{BS}} ira_3 + ta_2, \tag{A.2}$$

where r and t denotes the transmittance and reflection rate, respectively. We have $\eta = |r|^2$, and $|r|^2 + |t|^2 = 1$. In our scheme, the emitted single photon state code in ECC interact with the thermal noise through the object (BS), and the reflected signal is measured by single photon detectors. The initial state can be expressed as,

$$\rho_i = \prod_k \rho_1(k) \bigotimes \wp_{\text{th}} = \prod_k [\rho_1(k) \otimes \rho_{\text{th}}(k)]. \tag{A.3}$$

To calculate the the final state of ρ_i after scatting with BS, we can first calculate the repetitive element $\rho_1(k) \bigotimes \rho_{\text{th}}(k)$. Thus we have,

$$\begin{aligned}\rho = \rho_1 \bigotimes \rho_{\text{th}} &= |1\rangle_1 \langle 1| \bigotimes \sum_n p(n) |n\rangle_0 \langle n| = a_1^\dagger |0\rangle_1 \langle 0| a_1 \bigotimes \sum_n \frac{p(n)}{n!} a_0^{\dagger n} |0\rangle_0 \langle 0| a_0^n \\ &= \sum_n \frac{p(n)}{n!} a_1^\dagger a_0^{\dagger n} |00\rangle_{0,1} \langle 00| a_0^n a_1.\end{aligned} \tag{A.4}$$

After interaction with BS, we can obtain,

$$\begin{aligned}\rho &\xrightarrow{\text{BS}} \sum_n \frac{p(n)}{n!} (ira_2 + ta_3)^\dagger (ta_2 + ira_3)^{\dagger n} |00\rangle_{2,3} \langle 00| (ta_2 + ira_3)^n (ira_2 + ta_3) \\ \rho_f &= \sum_n \frac{p(n)}{n!} \sum_{k_1}^n C_n^{k_1} [(-ir)^{n-k_1} t^{k_1+1} a_2^{\dagger k_1} a_3^{\dagger n-k_1+1} + (-ir)^{n-k_1+1} t^{k_1} a_2^{\dagger k_1+1} a_3^{\dagger n-k_1}] \\ &\quad |00\rangle_{2,3} \langle 00| \sum_{k_2}^n C_n^{k_2} [(ir)^{n-k_2} t^{k_2+1} a_2^{k_2} a_3^{n-k_2+1} + (ir)^{n-k_2+1} t^{k_2} a_2^{k_2+1} a_3^{n-k_2}] \\ &= \sum_n \frac{p(n)}{n!} \sum_{k_1}^n C_n^{k_1} [(-ir)^{n-k_1} t^{k_1+1} \sqrt{k_1!(n-k_1+1)!} |k_1, n-k_1+1\rangle_{2,3} \\ &\quad + (-ir)^{n-k_1+1} t^{k_1} \sqrt{(k_1+1)!(n-k_1)!} |k_1+1, n-k_1\rangle_{2,3}] \\ &\quad \sum_{k_2}^n C_n^{k_2} [(ir)^{n-k_2} t^{k_2+1} \sqrt{k_2!(n-k_2+1)!} \langle k_2, n-k_2+1|_{2,3} \\ &\quad + (ir)^{n-k_2+1} t^{k_2} \sqrt{(k_2+1)!(n-k_2)!} \langle k_2+1, n-k_2|_{2,3}].\end{aligned} \tag{A.5}$$

We only care about the reflected photons, i.e. photons from the port 2. Trace the subspace of prot 3, we can obtain,

$$\begin{aligned}\rho_2 = &\sum_j^{n_k}\sum_{n_k}\frac{n_{\rm th}^{n_k}}{(n_{\rm th}+1)^{n_k+1}n_k!}\{C_{n_k}^j\eta^{n_k-j}(1-\eta)^j j!(n-j+1)![C_{n_k}^j(1-\eta)\\ &-C_{n_k}^{j-1}\eta]|j\rangle\langle j| + C_{n_k}^j\eta^{n_k-j+2}(1-\eta)^j(j+1)!(n-j)![C_{n_k}^j\eta\\ &-C_{n_k}^{j+1}(1-\eta)]|j+1\rangle\langle j+1|\}\\ =&\sum_{n_k}p'(n_k)|n_k\rangle\langle n_k|.\end{aligned} \tag{A.6}$$

According to our scheme, we only need to know the detection probability of single photon, i.e.

$$p'(1) = \frac{n_{\rm th}(1+n_{\rm th})(1-\eta)^2+\eta}{[1+(1-\eta)n_{\rm th}]^3}. \tag{A.7}$$

By performing projection measurements on a single photon detector array, we can get the corresponding detection probability with the response of object is there,

$$p(0|Y) = \left[\frac{n_{\rm th}}{1+(n_{\rm th})^2}\right]^d, \tag{A.8}$$

$$p(1|Y) = p'^d(1). \tag{A.9}$$

According to the general definition of SNR, we can obtain,

$${\rm SNR}_C = \left\{\frac{(1+n_{\rm th})^2[n_{\rm th}(1+n_{\rm th})(1-\eta)^2+\eta]}{n_{\rm th}[1+(1-\eta)n_{\rm th}]^3}\right\}^d. \tag{A.10}$$

It is obvious that ${\rm SNR}_C$ increases exponentially with dimension d.

For ECC scheme based on coherent state, we can use a similar method to calculate the SNR. The repetitive element is $|\alpha\rangle\langle\alpha|\bigotimes\rho_{\rm th}(k)$. Thus we have,

$$\begin{aligned}\rho \;=\; &|\alpha\rangle\langle\alpha|\bigotimes\sum_n p(n)|n\rangle_0\langle n| = \sum_n\frac{p(n)}{n!}D_1(\alpha)a_0^{\dagger n}|00\rangle_{0,1}\langle 00|a_0^n D_1^\dagger(\alpha).\\ \xrightarrow{\rm BS}&\sum_n\frac{p(n)}{n!}\sum_{k_1}^n C_n^{k_1}(-ir)^{n-k_1}t^{k_1}a_2^{\dagger k_1}a_3^{\dagger n-k_1}D_2(-ir\alpha)D_3(t\alpha)\\ &|00\rangle_{2,3}\langle 00|D_3^\dagger(t\alpha)D_2^\dagger(-ir\alpha)\sum_{k_2}^n C_n^{k_2}(ir)^{n-k_2}t^{k_2}a_2^{k_2}a_3^{n-k_2},\end{aligned} \tag{A.11}$$

where $D(\alpha)$ is the displacement operator. According to the general definition of SNR, we can obtain,

$${\rm SNR}_{coh} = \left\{\frac{(B-\eta)[(n_{\rm th}+1)e^{-\frac{|\alpha|^2\eta}{B}}(|\alpha|^2\eta+f_1)-|\alpha|^2B^3\eta e^{-|\alpha|^2\eta}]}{B^3n_{\rm th}}\right\}^d, \tag{A.12}$$

where $B = n_{\rm th}(1-\eta)+1$ and $f_1 = n_{\rm th}(1-\eta)[(|\alpha|^2-1)n_{\rm th}\eta+|\alpha|^2\eta+n_{\rm th}+1]$.

For EN scheme, the high-dimensional entangled states of auxiliary system A and system S are prepared.

$$|\Psi\rangle_{S,A} = \frac{1}{\sqrt{d}}\sum_k^d|1(k)\rangle_S|1(k)\rangle_A. \tag{A.13}$$

The photon emission of the system is interacted with the thermal environment through BS. The reflected signal is detected by joint measurement in the entangled state $|\Psi\rangle_{S,A}$. The initial state can be expressed as,

$$\begin{aligned}
\rho &= |\Psi\rangle_{S,A}\langle\Psi| \otimes \prod_k \sum_n p(n)|n(k)\rangle\langle n(k)|,\\
&= \frac{1}{d}\sum_k^d |1(k)\rangle_A|1(k)\rangle_S \sum_s^d \langle 1(s)|_A\langle 1(s)|_S \otimes \sum_n p(n)|n(k)\rangle\langle n(k)|\\
&\quad \otimes \sum_n p(n)|n(s)\rangle\langle n(s)| \otimes \prod_{k'\neq k,s}^d \sum_n p(n)|n(k')\rangle\langle n(k')|,\\
&= \frac{1}{d}\sum_{k,s}^d |1(k)\rangle_A\langle 1(s)| \otimes \sum_{nk,ns} p(nk)p(ns)|1(k)\rangle_S\langle 1(s)| \otimes |nk(k)\rangle\langle nk(k)|\\
&\quad \otimes |ns(s)\rangle\langle ns(s)| \otimes \prod_{k'\neq k,s}^d \sum_n p(n)|n(k')\rangle\langle n(k')|,\\
&= \frac{1}{d}\sum_{k,s}^d |1(k)\rangle_A\langle 1(s)| \otimes \sum_{nk,ns} \frac{p(nk)p(ns)}{nk!ns!} a_1^\dagger(k)a_0^{\dagger nk}(k)a_0^{\dagger ns}|\mathrm{vac}\rangle\langle\mathrm{vac}|\\
&\quad \otimes a_1(s)a_0^{nk}(k)a_0^{ns}(s) \otimes \prod_{k'\neq k,s}^d \sum_{nk'} p(nk')\frac{1}{nk'!}a_0^{\dagger nk'}(k')|\mathrm{vac}\rangle\langle\mathrm{vac}|a_0^{\dagger nk'}(k'). \qquad (A.14)
\end{aligned}$$

For the convenience of calculation, we divide the density operator into two cases: diagonal term and non-diagonal term. When $s = k$, after interact with BS, we can obtain,

$$\begin{aligned}
\rho &= \frac{1}{d}\sum_k^d |1(k)\rangle_A\langle 1(k)| \otimes \sum_n \frac{p(n)}{n!}a_1^\dagger(k)a_0^{\dagger n}(k)|\mathrm{vac}\rangle\langle\mathrm{vac}|a_1(k)a_0^n(k)\\
&\quad \otimes \prod_{k'\neq k}^d \sum_{nk'} p(nk')\frac{1}{nk'!}a_0^{\dagger nk'}|\mathrm{vac}\rangle\langle\mathrm{vac}|a_0^{\dagger nk'},\\
&\xrightarrow{\mathrm{BS}} \frac{1}{d}\sum_k^d |1(k)\rangle_A\langle 1(k)| \otimes \sum_n \frac{p(n)}{n!}[-ira_2^\dagger(k) + ta_3^\dagger(k)][-ira_3^\dagger(k) + ta_2^\dagger(k)]^n\\
&\quad |\mathrm{vac}\rangle\langle\mathrm{vac}|[ira_2(k) + ta_3(k)][ira_3(k) + ta_2(k)]^n\\
&\quad \otimes \prod_{k'\neq k}^d \sum_{nk'} \frac{p(nk')}{nk'!}[-ira_3^\dagger(k') + ta_2^\dagger(k')]^{nk'}|\mathrm{vac}\rangle\langle\mathrm{vac}|[ira_3(k') + ta_2(k')]^{nk'},\\
&= \frac{1}{d}\sum_k^d |1(k)\rangle_A\langle 1(k)| \otimes \sum_n \frac{p(n)}{n!}[-ira_2^\dagger(k) + ta_3^\dagger(k)]\\
&\quad \sum_{m1} C_n^{m1}t^{m1}(-ir)^{n-m1}a_2^{\dagger m1}(k)a_3^{\dagger n-m1}(k)|\mathrm{vac}\rangle\langle\mathrm{vac}|\\
&\quad \otimes [ira_2(k) + ta_3(k)]\sum_{m2} C_n^{m2}t^{m2}(ir)^{n-m2}a_2^{m2}(k)a_3^{n-m2}(k)\\
&\quad \otimes \prod_{k'\neq k}^d \sum_{nk'} \frac{p(nk')}{nk'!}[-ira_3^\dagger(k') + ta_2^\dagger(k')]^{nk'}|\mathrm{vac}\rangle\langle\mathrm{vac}|[ira_3(k') + ta_2(k')]^{nk'}.
\end{aligned}$$

In the joint measurement of the protocol, only the single photon state contributes. Ignoring the high excitation photon states, we can simplify the formula as follows.

$$\begin{aligned}
\rho &\xrightarrow{\mathrm{BS}} \frac{1}{d}\sum_k^d |1(k)\rangle_A\langle 1(k)| \otimes \sum_n \frac{p(n)}{n!}[C_n^0(-ir)^{n+1} + C_n^1t^2(-ir)^{n-1}]a_2^\dagger(k)a_3^{\dagger n}(k)\\
&\quad |\mathrm{vac}\rangle\langle\mathrm{vac}| \otimes a_2(k)a_3^n(k)[C_n^0(ir)^{n+1} + C_n^1t^2(ir)^{n-1}]\\
&\quad \otimes \prod_{k'\neq k}^d \sum_{nk'} \frac{p(nk')}{nk'!}r^{2nk'}a_3^{\dagger nk'}(k')|\mathrm{vac}\rangle\langle\mathrm{vac}|a_3^{nk'}(k'),\\
&= \frac{1}{d}\sum_k^d |1(k)\rangle_A\langle 1(k)| \otimes \sum_n p(n)[C_n^0(-ir)^{n+1} + C_n^1t^2(-ir)^{n-1}][C_n^0(ir)^{n+1}\\
&\quad + C_n^1t^2(ir)^{n-1}]|1(k),\, n(k)\rangle_{2,3}\langle 1(k),\, n(k)|\\
&\quad \otimes \prod_{k'\neq k}^d \sum_{nk'} p(nk')\eta^{nk'}|nk'(k')\rangle_3\langle nk'(k')|.
\end{aligned}$$

Trace the subspace of prot 3, we can obtain (define $R \equiv r^2$ and $T \equiv t^2$)

$$\rho_2 = \frac{1}{d}\sum_{k}^{d} p_1 |1(k)\rangle_A \langle 1(k)| \otimes |1(k)\rangle_2 \langle 1(k)| \otimes \prod_{k' \neq k}^{d} p_{\text{th}} |\text{vac}\rangle \langle \text{vac}|,$$

where

$$\begin{aligned} p_1 &= \sum_n p(n) R^{n-1} (nT - R)^2 \\ &= \frac{R(1 + Tn_{\text{th}})^2 - 2TRn_{\text{th}}(1 + Tn_{\text{th}}) + T^2 n_{\text{th}}(1 + n_{\text{th}} + Rn_{\text{th}})}{(1 + Tn_{\text{th}})^3}, \\ p_{\text{th}} &= \sum_n p(n) R^n \\ &= \frac{1}{1 + Tn_{\text{th}}}. \end{aligned}$$

Thus, in target recognition, the probability corresponding to the diagonal terms of density operator is

$$p_1(Y|1) = \frac{1}{d^2}\sum_{k}^{d} p_1 p_2^{d-1} = \frac{p_1 p_2^{d-1}}{d}.$$

When $s \neq k$, after interact with BS, we can obtain,

$$\begin{aligned} \rho &= \frac{1}{d}\sum_{k,s}^{d} |1(k)\rangle_A \langle 1(s)| \otimes \sum_{nk,ns} \frac{p(nk)p(ns)}{nk!ns!} a_1^{\dagger}(k) a_0^{\dagger nk}(k) a_0^{\dagger ns}(s) |\text{vac}\rangle\langle\text{vac}| \\ &\quad \otimes a_1(s) a_0^{nk}(k) a_0^{ns}(s) \otimes \prod_{k' \neq k,s}^{d} \sum_{nk'} p(nk') \frac{1}{nk'!} a_0^{\dagger nk'} |\text{vac}\rangle\langle\text{vac}| a_0^{\dagger nk'} \\ &\xrightarrow{\text{BS}} \frac{1}{d}\sum_{k,s}^{d} |1(k)\rangle_A \langle 1(s)| \otimes \sum_{nk,ns} \frac{p(nk)p(ns)}{nk!ns!} [-ira_2^{\dagger}(k) + ta_3^{\dagger}(k)][-ira_3^{\dagger}(k) \\ &\quad + ta_2^{\dagger}(k)]^{nk} [-ira_3^{\dagger}(s) + ta_2^{\dagger}(s)]^{ns} |\text{vac}\rangle\langle\text{vac}| [ira_2(s) + ta_3(s)][ira_3(s) \\ &\quad + ta_2(s)]^{ns} [ira_3(k) + ta_2(k)]^{nk} \otimes \prod_{k' \neq k}^{d} \sum_{nk'} \frac{p(nk')}{nk'!} [-ira_3^{\dagger}(k') + ta_2^{\dagger}(k')]^{nk'} \\ &\quad \otimes |\text{vac}\rangle\langle\text{vac}| \ [ira_3(k') + ta_2(k')]^{nk'}, \\ &= \frac{1}{d}\sum_{k,s}^{d} |1(k)\rangle_A \langle 1(s)| \otimes \sum_{nk,ns} \frac{p(nk)p(ns)}{nk!ns!} \sum_{k1} C_{nk}^{k1} [t^{k1}(-ir)^{nk-k1+1} \\ &\quad \times a_2^{\dagger k1+1}(k) a_3^{\dagger nk-k1}(k) + t^{k1+1}(-ir)^{nk-k1} a_2^{\dagger k1}(k) a_3^{\dagger nk-k1+1}(k)] \\ &\quad \otimes \sum_{s1} C_{ns}^{s1} t^{s1}(-ir)^{ns-s1} a_2^{\dagger k1}(k) a_3^{\dagger ns-s1}(k) |\text{vac}\rangle\langle\text{vac}| \\ &\quad \otimes \sum_{k2} C_{nk}^{k2} t^{k2}(ir)^{nk-k2} a_2^{k2}(k) a_3^{nk-k2}(k) \\ &\quad \otimes \sum_{s2} C_{ns}^{s2} [t^{s2}(ir)^{ns-s2+1} a_2^{s2+1}(s) a_3^{ns-s2}(s) + t^{s2+1}(ir)^{ns-s2} a_2^{s2}(s) a_3^{ns-s2+1}(s)] \\ &\quad \otimes \prod_{k' \neq k}^{d} \sum_{nk'} \frac{p(nk')}{nk'!} [-ira_3^{\dagger}(k') + ta_2^{\dagger}(k')]^{nk'} |\text{vac}\rangle\langle\text{vac}| \ [ira_3(k') + ta_2(k')]^{nk'}. \end{aligned}$$

Ignoring the high excitation photon states, we can simplify the formula as follows

$$\begin{aligned} \rho \xrightarrow{\text{BS}} &\frac{1}{d}\sum_{k,s}^{d} |1(k)\rangle_A \langle 1(s)| \otimes \sum_{nk,ns} \frac{p(nk)p(ns)}{nk!ns!} [C_{nk}^0 (-ir)^{nk+1} \\ &+ C_{nk}^1 t^2 (-ir)^{nk-1}] a_2^{\dagger}(k) a_3^{\dagger nk}(k) \otimes (-ir)^{ns} a_3^{\dagger ns}(s) |vac\rangle\langle vac| (ir)^{nk} a_3^{nk}(k) \\ &\otimes [(ir)^{ns+1} + \text{nt}^2 (ir)^{ns-1}] a_2(s) a_3^{ns}(s) \otimes \prod_{k' \neq k,s}^{d} \sum_{nk'} p(nk') R^{nk'} |nk'(k')\rangle_3 \langle nk'(k')|. \end{aligned}$$

Trace the subspace of prot 3, we can obtain,

$$\begin{aligned}\rho_2 = &\frac{1}{d}\sum_{k,s}^{d}|1(k)\rangle_A\langle 1(s)|\otimes\sum_{nk,ns}Rp(nk)p(ns)R^{nk-1}R^{ns-1}\\ &\times(Tnk-R)(Tns-R)|1(k)\rangle_2\langle 1(s)|\otimes\prod_{k'\neq k,s}^{d}p_{\rm th}|{\rm vac}\rangle\langle{\rm vac}|,\\ =&\frac{1}{d}\sum_{k,s}^{d}|1(k)\rangle_A\langle 1(s)|\otimes p_2|1(k)\rangle_2\langle 1(s)|\otimes\Pi_{k'\neq k,s}^{d}p_{\rm th}|{\rm vac}\rangle\langle{\rm vac}|,\end{aligned}$$

where

$$\begin{aligned}p_2 &= \sum_{nk,ns}p(nk)p(ns)RR^{nk-1}R^{ns-1}(Tnk-R)(Tns-R)\\ &= \frac{R}{(1+Tn_{\rm th})^4}.\end{aligned}$$

Thus, in target recognition, the probability corresponding to the non-diagonal terms of density operator is

$$p_2(Y|1) = \frac{1}{d^2}\sum_{k}^{d}\sum_{s}^{d-1}p_2p_{\rm th}^{d-2} = \frac{(d-1)p_2p_{\rm th}^{d-2}}{d}.$$

The corresponding detection probability with the response of object is there can be obtained as,

$$\begin{aligned}p(Y|\ 1) &= p_1(Y|\ 1)+p_2(Y|\ 1),\\ p(Y|\ 0) &= \frac{p(1)p_{\rm th}^{d-1}}{d}.\end{aligned}$$

The SNR of EN protocol is

$${\rm SNR}_E = \frac{1+(n_{\rm th})^{d+1}[n_{\rm th}(1+n_{\rm th})(1-\eta)^2+\eta d]}{n_{\rm th}[1+n_{\rm th}(1-\eta)]^{d+2}}. \tag{A.15}$$

It is obvious that SNR increases linearly with dimension d.

Appendix B. Evaluation of quantum Chernoff upper bound

The quantum Chernoff upper bound limits the asymptotic error probability. To evaluation this bound, we should trace the sate $\rho_{r0}^s\rho_{r1}^{1-s}$. To lowest order in η, $n_{\rm th}$ and using the general series expansion, we have,

$$\rho_{r0}^s = \prod_k(1-dn_{\rm th})^{sk}|{\rm vac}\rangle_k\langle{\rm vac}| + n_{\rm th}^sI_k, \tag{B.1}$$

where $I_k = \sum_j|j\rangle_k\langle j|$ is the identity operator on the single photon subspace.

$$\rho_{r1}^{1-s} = \prod_k(1-\eta-dn_{\rm th})^{1-s}|{\rm vac}\rangle_k\langle{\rm vac}| + n_{\rm th}^{1-s}(I_k-|\psi\rangle_k\langle\psi|)+(n_{\rm th}+\eta)^{1-s}|\psi\rangle_k\langle\psi|. \tag{B.2}$$

The quantum Chernoff bound takes the form

$$Q_C = \min_{s\in[0,1]}{\rm tr}\rho_{r0}^s\rho_{r1}^{1-s} = \min_{s\in[0,1]}(1-\eta)^{(1-s)d}\left\{1+n_{\rm th}[-1+\left(1+\frac{\eta}{n_{\rm th}-\eta n_{\rm th}}\right)^{1-s}]\right\}^d. \tag{B.3}$$

According to the [4], the quantum Chernoff bound of entanglement protocol takes the form

$$Q_E = \min_{s\in[0,1]}(1-\eta)^{1-s}\left\{1+\frac{n_{\rm th}}{d}[-1+\left(1+\frac{\eta d}{n_{\rm th}-\eta n_{\rm th}}\right)^{1-s}]\right\}. \tag{B.4}$$

In the express of Q, ${\rm tr}\rho_{r0}^s\rho_{r1}^{1-s}$ is a function of $s\in[0,\ 1]$. Its minimum value depends on the parameters d, η and $n_{\rm th}$, which is shown in figure B1. The minimum values for different parameters are appear around $s=0.5$.

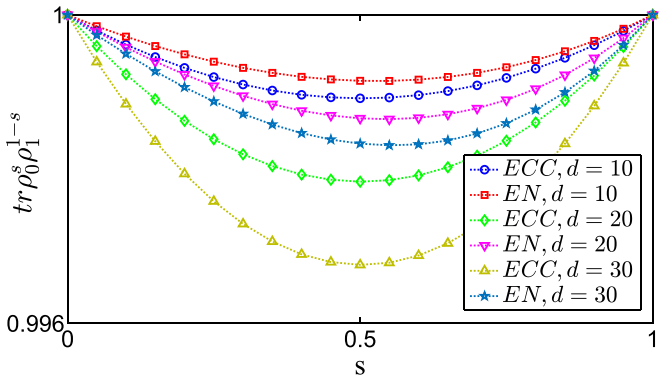

Figure B1. $\mathrm{tr}\rho_{r0}^{s}\rho_{r1}^{1-s}$ as a function of s with different auxiliary dimension d and schmems. The reflection rate $\eta = 0.01$, the thermal noise $n_{\mathrm{th}} = 0.1$.

Appendix C. The detection SNR for different error correction schemes

By using ECC, the receiver could discover and correct the coding errors with it spontaneously during the transmission. The redundant information in the ECC usually be used to against the environmental noise due to the self-corrective characteristics. In our scheme, we only need to identify the signal photon is reflected to the receiver or not. Thus, it is necessary for us to enlarge the code distance d (the number of the code elements) to better distinguish the state $|0\rangle$ and $|1\rangle$. By using the law of large numbers, the receiver have the ability to correct k error codes after transmission. k satisfies $k \leqslant (d-1)/2$. The corresponding detection probability is

$$p_0(k) = \sum_{s=0}^{k} \mathrm{C}_d^s p_0^{d-s} p_1^s, \tag{C.1}$$

$$p_1(k) = \sum_{s=0}^{k} \mathrm{C}_d^s p_1^{d-s} p_0^s, \tag{C.2}$$

where p_1 and p_0 denotes the single detector response probability of state $|0\rangle$ and $|1\rangle$, respectively. In ECC, all codes except the discriminant codes given by the protocol are regarded as forbidden codes, which will be discarded in detection. Thus, in signal detection, the probability satisfies $p_0(k) + p_0(k) \leqslant 1$.

As shown in figure C1, we exam the effects of k and d on SNR and p. In figures C1(a) and (b), we set $d = 20$, SNR decreases and p increases with the increase of k. In figures C1(c) and (d), we use symmetric coding protocol to detect the reflected signal, where $k = \mathrm{Round}[(d-1)/2]$. It is shown that, with the increase of d, SNR increases obviously, and p decreases. This conclusion is consistent with the section 4. Therefore, if we need a higher SNR, we need to select $k = 0$, and if we need a higher detection efficiency, we need to select $k = \mathrm{Round}[(d-1)/2]$.

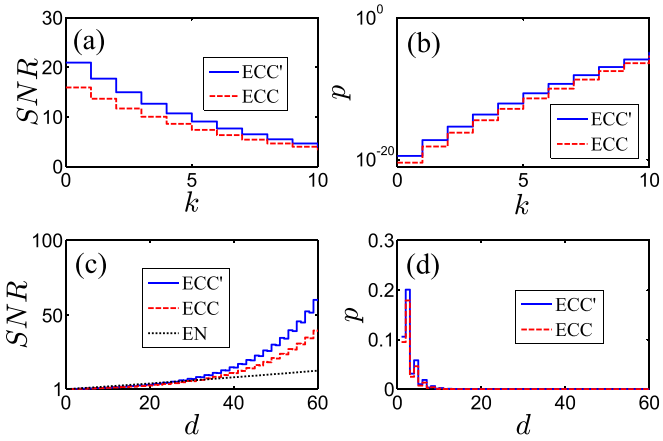

Figure C1. SNR and p as a function of k and d. Figure note 'ECC' denotes the ECC protocol for single photon detection, 'ECC' denotes the improved ECC protocol, and 'EN' denotes the entanglement protocol. The reflection rate $\eta = 0.02$, the thermal noise $n_{\mathrm{th}} = 0.1$.

In addition, one should notice that, perform N times measurement is not equivalent to using ECC. The SNR means the total signal detected over the total noise. Meanwhile, the environmental noise has always played an important role during each detection process. Thus, the noise increases with the increasing of the signal, this may keep the SNR unchanged. For EN scheme, as long as the received signal contains the entanglement, it can be regarded as a signal. Under the condition $1 \gg p(Y|1) > p(Y|0)$, emitting N copies of entangled states at one time, we can obtain that,

$$\begin{aligned} \mathrm{SNR}_E^{(N)} &= \frac{1-[1-p(Y|1)]^N}{1-[1-p(Y|0)]^N} \\ &= \frac{N\times p(Y|1)+O[-p(Y|1)]^2}{N\times p(Y|0)+O[-p(Y|0)]^2} \\ &\leqslant \frac{N\times p(Y|1)}{N\times p(Y|0)} = \mathrm{SNR}_E. \end{aligned} \tag{C.3}$$

Thus, a large number of copies of the initial state can not enhance the SNR ratio.

Appendix D. Detection efficiency of two different protocols

Detection efficiency is an important evaluation criterion like SNR to indicate the ability of the detection system. Realistically, detection efficiency should combine with the detection scheme, i.e. the cost of quantum resources in target recognition. For our scheme, the required resource is single-photon state, and for entanglement scheme, the required resources is entanglement state. At present, spontaneous parametric down-conversion and spontaneous four-wave mixing provide the best available sources of heralded single photons. The reported conversion efficiency for 710 nm laser is $pc_c \approx 10^{-5}$ in [37]. And the most efficient way to generate polarization-entangled photon pairs is to use type-II phase-matched spontaneous parametric down-conversion. The corresponding conversion efficiency is $pc_e \approx 10^{-12}$ for 775 nm pump pulse in [38]. Assuming that the receiving of the detector is 1 second each time, the number of photons reach to the receiver per unit power is

$$Rc = \frac{p_{\mathrm{in}}t}{c/\lambda h}pc \times p\frac{1}{p_{\mathrm{in}}} = \frac{t}{c/\lambda h}pc \times p, \tag{D.1}$$

where pc denotes the conversion efficiency $\{pc_c, pc_e\}$, λ denotes the wavelength of the laser $\{710,775\}$-nm, p denotes the detection efficiency $\{p_C', p_E\}$. Put the parameters in [37, 38] into the above formula, we can obtain $Rc_c \approx 4 \times 10^{13}p_C'$ W^{-1} s^{-1} and $Rc_e \approx 4 \times 10^{6}p_E$ W^{-1} s^{-1}.

ORCID iDs

Wen-Zhao Zhang https://orcid.org/0000-0001-7885-4282
Yu-Han Ma https://orcid.org/0000-0001-9768-9171
Jing-Fu Chen https://orcid.org/0000-0002-7207-969X

References

[1] Jin G R, Yang W and Sun C P 2017 *Phys. Rev.* A **95** 013835
[2] Cai Y and Zhu S Y 2005 *Phys. Rev.* E **71** 056607
[3] Brida G, Genovese M and Ruo Berchera I 2010 *Nat. Photon.* **4** 227–30
[4] Lloyd S 2008 *Science* **321** 1463–5
[5] Barzanjeh S, Guha S, Weedbrook C, Vitali D, Shapiro J H and Pirandola S 2015 *Phys. Rev. Lett.* **114** 080503
[6] Tan S H, Erkmen B I, Giovannetti V, Guha S, Lloyd S, Maccone L, Pirandola S and Shapiro J H 2008 *Phys. Rev. Lett.* **101** 253601
[7] Chang C W S, Vadiraj A M, Bourassa J, Balaji B and Wilson C M 2019 *Appl. Phys. Lett.* **114** 112601
[8] Barzanjeh S, Pirandola S, Vitali D and Fink J M 2019 arXiv:1908.03058
[9] Pirandola S and Lloyd S 2008 *Phys. Rev.* A **78** 012331
[10] Pirandola S, Bardhan B R, Gehring T, Weedbrook C and Lloyd S 2018 *Nat. Photon.* **12** 724–33
[11] Sanz M, Las Heras U, García-Ripoll J J, Solano E and Di Candia R 2017 *Phys. Rev. Lett.* **118** 070803
[12] Wilde M M, Tomamichel M, Lloyd S and Berta M 2017 *Phys. Rev. Lett.* **119** 120501
[13] Lopaeva E D, Ruo Berchera I, Degiovanni I P, Olivares S, Brida G and Genovese M 2013 *Phys. Rev. Lett.* **110** 153603
[14] Las Heras U, Di Candia R, Fedorov K G, Deppe F, Sanz M and Solano E 2017 *Sci. Rep.* **7** 9333
[15] Xiong B, Li X, Wang X Y and Zhou L 2017 *Ann. Phys.* **385** 757–68
[16] Liu K, Zhang Q W, Gu Y J and Li Q L 2017 *Phys. Rev.* A **95** 042317
[17] Spedalieri G and Braunstein S L 2014 *Phys. Rev.* A **90** 052307
[18] Zhuang Q, Zhang Z and Shapiro J H 2017 *J. Opt. Soc. Am.* B **34** 1567
[19] Pirandola S, Laurenza R, Lupo C and Pereira J L 2019 *NPJ Quantum Inf.* **5** 50
[20] De Palma G and Borregaard J 2018 *Phys. Rev.* A **98** 012101

[21] Zhuang Q, Zhang Z and Shapiro J H 2017 *Phys. Rev.* A **96** 020302
[22] Deng F G and Long G L 2004 *Phys. Rev.* A **69** 052319
[23] Schlingemann D and Werner R F 2001 *Phys. Rev.* A **65** 012308
[24] Israel Y, Rosen S and Silberberg Y 2014 *Phys. Rev. Lett.* **112** 103604
[25] Malik M, Magaña-Loaiza O S and Boyd R W 2012 *Appl. Phys. Lett.* **101** 241103
[26] Ray S, Schneeloch J, Tison C C and Alsing P M 2019 *Phys. Rev.* A **100** 012327
[27] Chernoff H 1952 *Ann. Math. Stat.* **23** 493–507
[28] Audenaert K M R, Calsamiglia J, Muñoz Tapia R, Bagan E, Masanes L, Acin A and Verstraete F 2007 *Phys. Rev. Lett.* **98** 160501
[29] Calsamiglia J, Muñoz Tapia R, Masanes L, Acin A and Bagan E 2008 *Phys. Rev.* A **77** 032311
[30] Jozsa R 1994 *J. Mod. Opt.* **41** 2315–23
[31] Cook C E and Bernfeld M 1967 *Radar Signals: An Introduction to Theory and Application* (New York: Academic)
[32] Farina A 1992 *Antenna-Based Signal Processing Techniques for Radar Systems* (Boston, MA: Artech House)
[33] Skolnik M I 2008 *Radar Handbook* 3rd edn (New York: McGraw-Hill)
[34] Shor P W and Preskill J 2000 *Phys. Rev. Lett.* **85** 441–4
[35] Calderbank A R and Shor P W 1996 *Phys. Rev.* A **54** 1098–105
[36] Ma Y H, Xu D, Dong H and Sun C P 2018 *Phys. Rev.* E **98** 022133
[37] Langford N K, Ramelow S, Prevedel R, Munro W J, Milburn G J and Zeilinger A 2011 *Nature* **478** 360–3
[38] Zhu E Y, Tang Z, Qian L, Helt L G, Liscidini M, Sipe J E, Corbari C, Canagasabey A, Ibsen M and Kazansky P G 2012 *Phys. Rev. Lett.* **108** 213902